23rd AIAA Applied Aerodynamics Conference
6 - 9 June 2005, Toronto, Ontario Canada

AIAA 2005-5216

A Conceptual Design Methodology for Predicting the Aerodynamics of Upper Surface Blowing on Airfoils and Wings

Ernest B. Keen* and William H. Mason**
Department of Aerospace & Ocean Engineering
Virginia Polytechnic Institute and State University
Blacksburg, VA 24061

An aerodynamic analysis methodology for Upper Surface Blowing aerodynamics is presented. This methodology is useful for aerodynamic estimation in the conceptual and preliminary design phases of USB or USB/Distributed Propulsion aircraft concepts. Analytical flow models together with an examination of some two-dimensional experimental data is used to establish the method. The method was then extended to treat fully 3-D wings. Comparisons of the method with experimental data from wind tunnel and flight-testing of USB designs demonstrates its usefulness. Finally, a brief comparison was done with an existing Vortex Lattice Method for USB wings, and the current method demonstrated good agreement.

Nomenclature

b_{USB}	=	span of upper surface blowing (ft)
c	=	local chord of airfoil (ft)
c_f	=	chord of trailing edge flap (ft)
C_j,C_μ	=	sectional blowing coefficient/momentum flux coefficient
C_l	=	sectional lift coefficient
C_d	=	sectional drag coefficient
C_{dp}	=	sectional pressure drag coefficient
C_m	=	sectional pitching moment coefficient, about quarter-chord
E	=	ratio of flap chord to local airfoil chord = c_f/c
FF	=	form factor for friction drag estimation
$\dot{m}$	=	mass flow rate of engine
p	=	static pressure (lb/ft^2)
R	=	radius of curvature (ft)
V_∞	=	freestream velocity (ft/s)
V_{jet}	=	engine exhaust jet velocity (ft/s)
α	=	angle of attack (wing and airfoil) (rad)
δ_f	=	USB flap deflection, relative to chord line (rad)
γ	=	parabolic camber, percent of chord
ζ	=	pressure drag factor

I. Introduction

One of the most promising powered-lift concepts is Upper Surface Blowing (USB), where the engines are placed above the wing and the exhaust jet becomes attached to the upper surface. The jet thrust can then be vectored by use of the trailing edge curvature using flaps, since the jet flow tends to remain attached by the "Coanda Effect".

* Member, AIAA
** Professor, Associate Fellow, AIAA

Wind tunnel and flight testing have shown USB aircraft to be capable of producing maximum lift coefficients near 10[1-3]. They have the additional benefit of the wing shielding the engine noise from the ground[4].

Given the potential performance benefits from USB aircraft, one would expect that conceptual design methods exist for their development. This is not the case however. While relatively complex solutions are available[5,6], there is currently no adequate low-fidelity methodology for use in the conceptual and preliminary design of USB or USB/distributed-propulsion aircraft[7]. The focus of the current work is to provide such a methodology for conceptual design of USB aircraft. The method relies on existing and new theoretical flow models and limited two-dimensional experimental data, and shown here to compare well with a wide range of configuration wind tunnel data. This semi-analytical method and can be integrated into existing aircraft design software. The complete details are contained in the thesis by Keen[8].

The paper begins with a basic discussion of airfoil theory extended to include blowing effects. This is followed by a description of the 2-D model for USB predictions and the necessary correlation of this model with experimental data. The process of obtaining predictions for 3-D USB wings is then presented along with comparisons with experimental data using the current methodology.

II. Airfoil Theory Extended to Include Blowing

First, it is important to describe the aerodynamic effects induced in a flowfield by the introduction of blowing. The correlating parameter we will use is the familiar blowing coefficient or jet momentum coefficient:

$$C_\mu = C_j = \frac{\dot{m} V_{jet}}{q_\infty c} \tag{1}$$

where the numerator is the gross thrust of a propulsion system at design condition. As described by Spence[9], there are two ways in which blowing will alter the performance of an airfoil:

1. Through the direct reaction of jet momentum leaving the trailing edge
2. Through the change in airfoil circulation induced by the jet, i.e. through the changes induced in the surface pressures around the airfoil.

The first is clear, while the second, as will be shown, can be complicated. It involves many separate effects that are dependent on a wide array of flow features.

A. Kutta-Joukowski Theorem for Blown Sections

It is helpful to re-derive the Kutta-Joukowski theorem as it applies to these cases. Consider the situation of a self-propelled, 2-D wing in a uniform, steady flow. We will ignore body forces and assume that the propulsion system operates at design condition. A representative sketch of the body and control volume is given below in Figure 1.

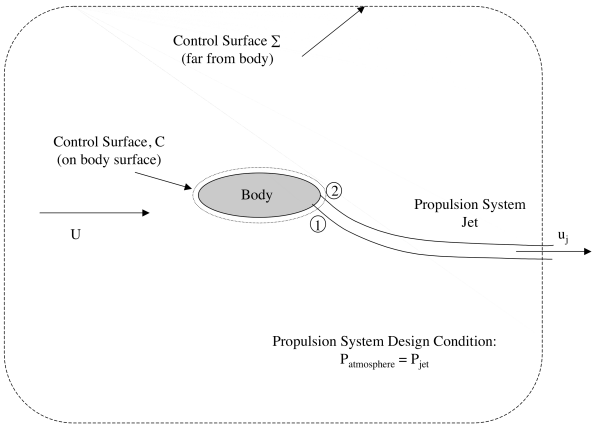

Figure 1. Sketch of control volumes for self-propelled airfoil

For self-propelled bodies, we generate forces by surface pressures and reaction forces. Following the general derivation from Karamcheti[10], the force on this body is:

$$\mathbf{F} = -\oint p\mathbf{n}dc - \dot{m}\left(u_j - U_\infty\right)\mathbf{i} \tag{2}$$

where p is the pressure, dc is a differential length along a control surface, and $\mathbf{n}$ is the unit normal to the surface. The full derivation is not shown here, but is analogous to that done in Ref. 10 with special attention to boundary conditions on the body. We find that the total force on the body can be written as:

$$\mathbf{F} = \rho_\infty U_\infty \Gamma_{\text{mod}}\mathbf{k} + \rho_\infty U_\infty \left(u_j t \sin\delta\right)\mathbf{k} - \dot{m}\left(u_j - U_\infty\right)\mathbf{i} \tag{3}$$

where Γ_{mod} reflects the super-circulation induced by the jet, and the second term represents the vertical reaction lift of the jet.

This is the analogy to the Kutta-Joukowski theorem for a self-propelled body. It simply states that the jet will modify the basic circulation (super-circulation), the pressure on any surface on which it flows, and will produce a net thrust. A derivation by Siestrunck[11] results in a similar expression.

B. The Kutta Condition

The presence of a jet at the trailing edge, or leaving the trailing edge, affects the circulation around the airfoil. The jet functions almost as a solid extension of the airfoil and thus induces chord loadings similar to a mechanical flap, and there is also a change in the Kutta condition at the trailing edge. The curvature of the jet sheet allows it to support a pressure difference across it, and thus in a typical situation the pressure at the trailing edge on the upper surface is lower than that on the lower surface. Having the jet sheet at the trailing edge effectively relaxes the classical Kutta condition, allowing the upper surface and lower surface to come to different velocities at the trailing edge (i.e. allowing a ΔC_p at the TE). Siestrunck[10] says, "The thin jet sheet plays the part of a regulator of the circulation as would the sharp trailing edge of a solid flap". Thus, the adverse pressure gradient on the upper surface is relived or even changed to a favorable one. This is an increase in circulation. This effect could be seen even if the jetflap angle were zero.

III. Two-Dimensional Model for USB

Based on a survey of the literature available for upper surface blowing, and powered-lift in general, it is clear that the classic jet-flap theory from Spence[9] is inadequate for upper surface blown configurations. However, studies have been published by Hough[12] showing that the "jet-flap analogy" can be very useful in predicting lift and pitching moment *increments* due to changes in geometry or flight state.

As confirmed by Hough and others, we expect that jet-flap theory under-predicts the total lift and pitching moment because it does not take into account the interaction between the wing and the jet, nor the general viscous nature of the jet flow. Knowing this, if we can estimate the surface pressures for those areas wetted by the jet, the total forces could be approximated much better. It was found that Circular Streamline Theory (CST), introduced in this paper, provides a good approximation and is very easy to use. In addition, empirical relations were developed to approximate viscous losses and beneficial effects from entrainment.

A. Spence's Jet-Flap Theory

Classical Jet-Flap theory refers to the inviscid development by Spence[9,13] in the 1950s. His original work was for inviscid, incompressible flow past a thin, 2-D wing at moderate incidence with a thin jet exhausting from the trailing edge. It was later extended to include cases where the jet enters the flow tangentially along a deflected flap, and for cases with section camber by Davis[14]. The details of the problem will not be presented, only the resulting equations.

Since this is a linear problem, the total solution can be viewed as a superposition of individual effects. The sectional lift coefficient is given by Eqn (4).

$$C_l = 2\pi\alpha + 4\pi B_o\alpha + 2\left(\chi + \sin\chi + 2\pi D_o\right)\delta_f + 4\pi\gamma\left(1 + C_o\right) \tag{4}$$

Note that χ is a "flap parameter" defined by Spence as:

$$\chi = 2\sin^{-1}\sqrt{E} \tag{5}$$

The coefficients B_o and C_o are empirical functions of the blowing coefficient. The following curve fits were provided by the respective authors for these coefficients:

$$\begin{aligned} B_o &= 0.0917C_\mu^{1/2} + 0.0880C_\mu + 0.0041C_\mu^{3/2} \\ C_o &= 0.0600C_\mu^{1/2} + 0.4499C_\mu - 0.0922C_\mu^{3/2} \end{aligned} \tag{6}$$

The coefficient D_o is a more involved function of C_μ and E and was not provided by Spence. A good curve fit was calculated as part of the current work:

$$D_o = A_o + \frac{-1.931E^{1/4}}{4\pi}\left(C_\mu^{(-0.9621E^2 + 0.5785E + 0.1639)}\right) \tag{7}$$

where:

$$A_o = 0.2817C_\mu^{1/2} + 0.0259C_\mu + 0.0124C_\mu^{3/2} \tag{8}$$

Similarly, Spence worked with the sectional pitching moment coefficient. Again using superposition of solutions, the general form of the pitching moment equation is:

$$C_{m,le} = \left(-\frac{1}{2}\pi + E_o\right)\alpha - \left(\frac{1}{2}\chi + \sin(\chi) + \frac{1}{4}\sin(2\chi)\right)\delta_f + G_o\delta_f \tag{9}$$

where E_o was given explicitly by Spence, but a curve fit for G_o was found in the course of this work. Generally G_o is a function of C_μ and E, but since most flaps are roughly 30% of the section chord, it was reduced to only a function of C_μ:

$$\begin{aligned} E_o &= -0.3057C_\mu^{1/2} - 0.2466C_\mu + 0.0406C_\mu^{3/2} \\ G_o &= -0.3318C_\mu^{1/2} - 1.0332C_\mu + 0.0842C_\mu^{3/2} \end{aligned} \tag{10}$$

Given the pitching moment about the leading edge and the section lift coefficient, the moment can be transferred to the quarter chord location.

$$C_{m,0.25c} = \frac{1}{4}C_l + C_{m,le} \tag{11}$$

Equations (4) through (11) complete our use of the jet-flap theory. Since it is based on 2-D thin-airfoil theory (note that all equations reduce to the classic formulas when there is no blowing) we cannot predict any drag force from this theory.

B. Circular Streamline Theory (CST)

To estimate the surface pressures induced by the jet on the curved aft surface we formulated a method using circular streamline theory. We consider that while the mechanism of coanda flow is turbulent momentum transfer

within the jet, the nearly circular streamlines it creates can be characterized by potential flow. Consider the potential flow induced by a point vortex shown in Figure 2.

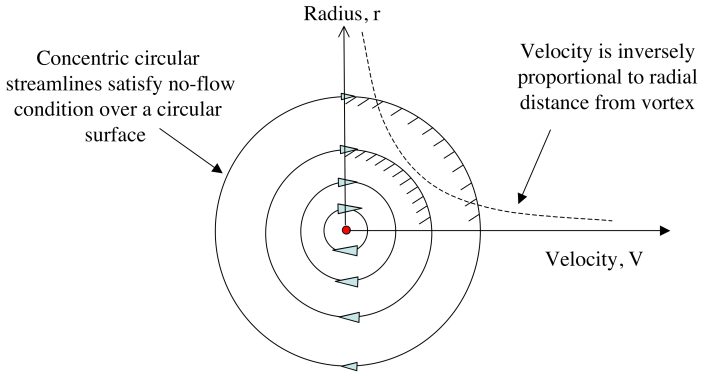

Figure 2. Illustration of a point vortex and associated streamlines

Any of the streamlines in this figure could easily be viewed as solid surfaces, and the flow will behave locally as if it were induced by a point vortex.

Based on this idea, the velocity profile of a wall jet in an external stream flowing over a curved surface could be described by a uniform flow and a point vortex. Figure 3 illustrates this.

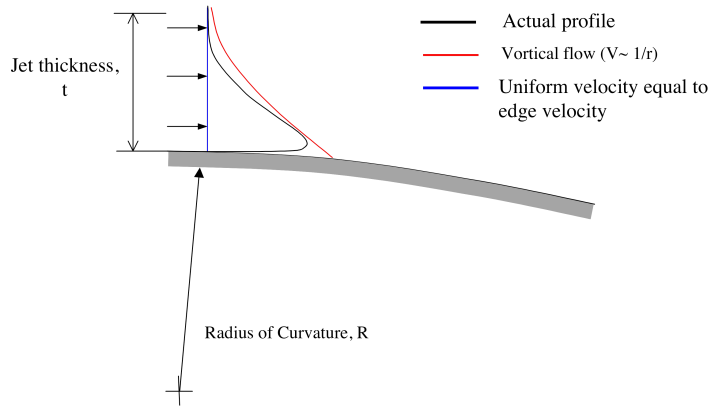

Figure 3. Wall jet velocity profile approximation

The velocity from potential theory is:

$$V = U_e(x) - \frac{\Gamma_{PV}}{2\pi r} \tag{12}$$

where Γ_{PV} represents a point vortex strength. Using this velocity in Bernoulli's equation and taking the derivative w.r.t. radius, r:

$$\frac{dp}{dr} = \rho_{jet}\left(\frac{\Gamma_{PV}^2}{4\pi^2 r^3} - \frac{\Gamma_{PV} U_e}{2\pi r^2}\right) \tag{13}$$

The ODE in equation (13) is integrable, and we integrate from R (surface) and $R+t$ (the edge of the jet) and get:

$$p_w - p_{localstatic} = \frac{\rho_{jet}\Gamma_{PV}^2}{2(4\pi^2)}\left(\frac{1}{(R+t)^2} - \frac{1}{R^2}\right) - \frac{\rho_{jet}\Gamma_{PV} U_e}{2\pi}\left(\frac{1}{R+t} - \frac{1}{R}\right) \tag{14}$$

We use the known value of the nozzle exit velocity, V_{exit}, to substitute for Γ_{PV} in terms of V_{exit} and a reference radius, R_{ref} (taken from here forward to be $R+t/2$). In addition, the average jet velocity will be altered by the external flow. For simplicity, say that it assumes a roughly constant value of nV_{exit} as it flows over the surface, where n is a constant of O(1). This gives:

$$\Delta p = (p_{\substack{local \\ static}} - p_\infty) + \frac{\rho_{jet}}{2} R_{ref}^2 (U_e - nV_{exit})^2 \left(\frac{1}{(R+t)^2} - \frac{1}{R^2} \right) - \rho_{jet} R_{ref} U_e (U_e - nV_{exit}) \left(\frac{1}{R+t} - \frac{1}{R} \right) \tag{15}$$

To use this formulation in practice, it is easiest to discretize the surface into short segments where the local pressure is found from surface curvature and equation (15). This idea is shown in Figure 4.

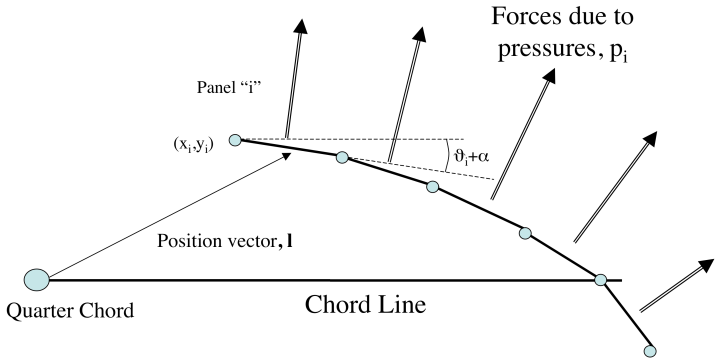

Figure 4. Discretized aft surface for CST

The forces and moments are then simple summations involving the orientation, surface pressure, and length of each segment.

C. Drag Estimation

In two-dimensions, the drag sources present for a subsonic airfoil are the skin friction drag and the pressure drag. Pressure drag for a typical airfoil comes from separated flow, which is usually not an issue when blowing is used. As seen in the previous section, however, there is a pressure force from the jet that acts as drag. The remaining component is skin friction, which was estimated in the standard manner using a form factors approach with empirical data.

The skin friction is accounted for using a form factors approach similar to that presented by Mason[15] and Torenbeek[16]. In this case the portion of the surface wetted by the jet has a different skin friction coefficient. The friction drag coefficient (part of C_{do}) is:

$$C_d = \left(C_{F,fs} \left(\frac{S_{fs}}{S_{ref}} \right) + C_{F,jet} \left(\frac{S_{jet}}{S_{ref}} \right) \right) FF \tag{16}$$

where C_F is a skin friction coefficient and S is a wetted area. The subscripts "*fs*" and "*jet*" denote the separate portions of the airfoil surface wetted by the jet exhaust and the "standard" flow.

The drag due to the jet pressure described in the previous section will not all be realized. In fact, a large portion of it can and will be balanced by leading edge suction. A simple multiplier, ζ, can be applied to the pressure drag in that respect. The determination of the magnitude of this multiplier must be empirically based.

D. Entrainment Effects

The effects of entrainment are more difficult to quantify. At this point, there is no established method for incorporating these types of effects for upper surface blown configurations. The goal of this work is only to provide enough empirical approximations for these effects to correlate existing data. A set of experiments designed to measure entrainment effects within the framework of the current prediction method would be the next logical step, but has not been done here.

Essentially, we want to find the lift augmentation produced by direct fluid entrainment from the jet. For small amounts of blowing, we should also account for the positive lift and drag effects produced by boundary layer control. A multiplicative factor is used on the lift to account for entrainment effects. We call this factor, η_{ent}. While the choice of these factors can be subjective and/or sensitive to configuration, we will show that good correlation can be obtained via relatively simple empirical relations.

IV. Correlation with 2-D Experimental Data

Correlation of the 2-D methodology was done using experimental results from the University of Texas at Arlington. Full details of these experiments can be found in theses by Roberts[17], Pernice[18], and Jeon[19]. They used a modified, symmetric NACA airfoil with a propulsive nozzle located on the aft portion of the upper surface. The lift and pitching moments were recorded for various angles of attack and C_j's. Empirical factors present in the methodology (n, η_{ent}, ζ) were adjusted to provide good correlation up to C_j=10.

Experimental values of the section lift coefficient are shown in Figure 5 for a range of angles of attack. Also shown are the values obtained using the current method after correlation.

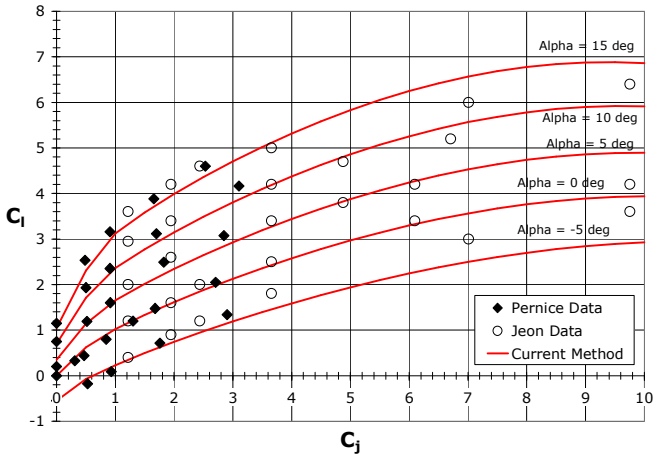

Figure 5. Section lift coefficient vs. blowing coefficient

The primary focus was on correlation of the sectional lift coefficient and the sectional pitching moment was correlated without additional work. A sample of the correlation is shown in Figure 6:

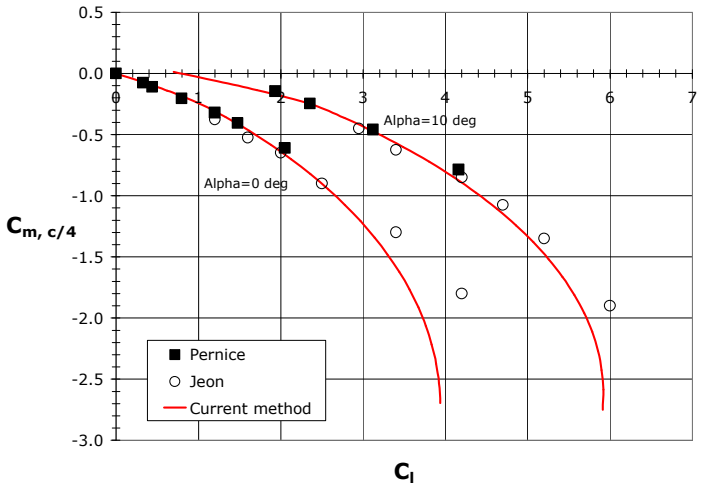

Figure 6. Section pitching moment coefficient vs. section lift coefficient

Note that the correlation appears to break down for large values of the blowing coefficient. While most practical designs would not operate much in this region, adjustments would be necessary to use the current method for very large blowing coefficients.

V. Three-Dimensional Predictions

Calculations of the 3-D performance were carried out by the use of a computer program called the "High-Lift Module". This program uses a modified Weissinger lifting line method and was created by researchers at the University of California at Davis. More information on the modified Weissinger method and the program itself can be found in work by Paris[20]. The 2-D polars calculated using the process described above are used directly in the High-Lift Module.

One critical distinction necessary to go from 2-D to 3-D calculation lies in the definition of the blowing coefficient. Since it is defined as the momentum flux of the jet leaving the trailing edge per unit span, our new definition should include an appropriate span of blowing.

$$C_j = \frac{\dot{m}V_{exit}}{q_\infty c b_{USB}} \approx \frac{\text{Gross Thrust}}{q_\infty c b_{USB}} \tag{17}$$

Once the method finds the 2-D USB polars and appropriate non-blown polars and the user defines where each applies, the lift, drag, and pitching moments of the wing can be calculated. Comparisons were performed for the current methodology with experimental data taken from wind tunnel versions of USB configurations. It was found that the lift coefficient correlated very well, but were highly dependent on the propulsion system model used. The pitching moment also correlated well. Though the magnitude was too large for large values of flap deflection, $C_{m\alpha}$ was predicted well. The drag did not correlate as well due to a lack of 2-D data for correlation, and due to numerical solver problems in the High-Lift module that produced erroneously large values for induced drag.

A. Comparison with NASA TN D-7526[21]

This set of experiments investigated the longitudinal aerodynamics of a large-scale, 2-engine USB configuration. Figure 8 describes the model used and relevant features:

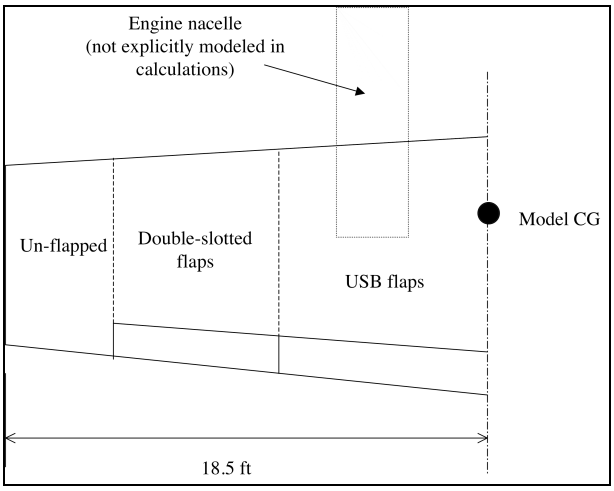

Figure 7. Sketch of wind tunnel model used in experiments of Ref. 21

General agreement of the current method with experimental data was good, particularly for the lift. Figures 8 and 9 show the lift and pitching moments versus angle of attack for a sample case with USB flaps deflected 20 degrees.

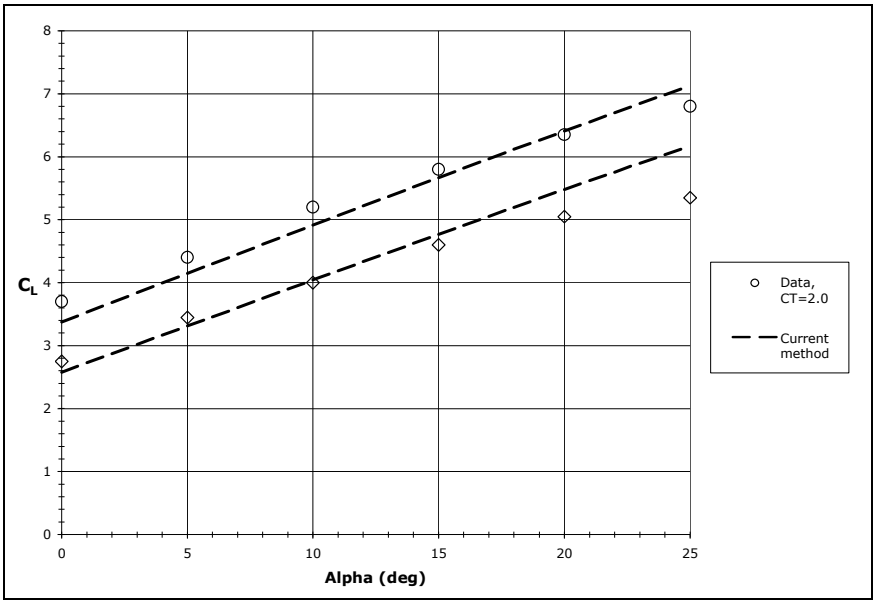

Figure 8. Comparison of C_L with experiment

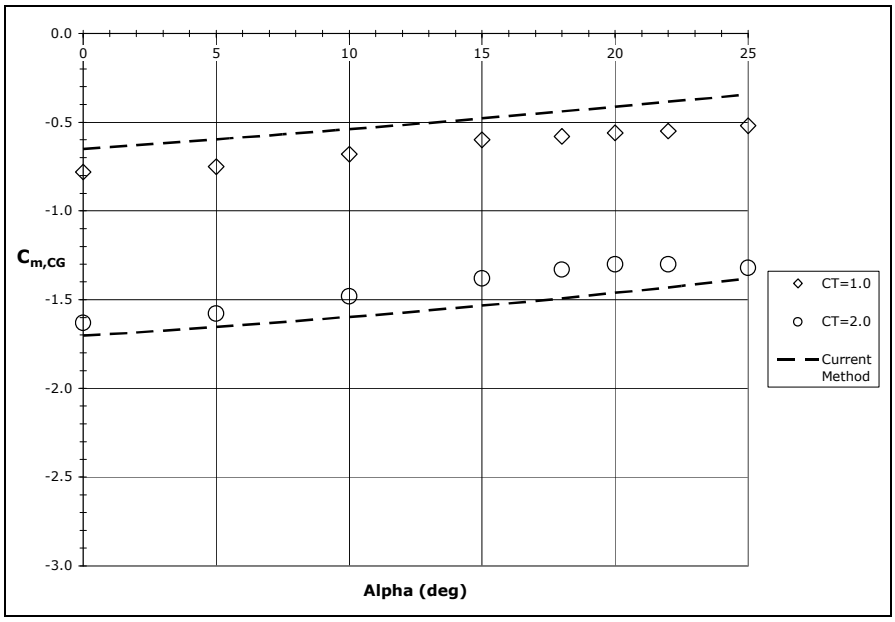

Figure 9. Comparison of $C_{m,CG}$ with experiment

Due to numerical problems in the High Lift Module arising because of the drastic variation of the 2-D polars across the span, the calculated spanload had large spanload oscillations near the edge of the USB flaps. These oscillations caused the induced drag to be too high. Based on the experimental data, a correction factor was developed for use in calculateing drag. Figure 10 shows the corrected values against experiment for 20 degrees flaps:

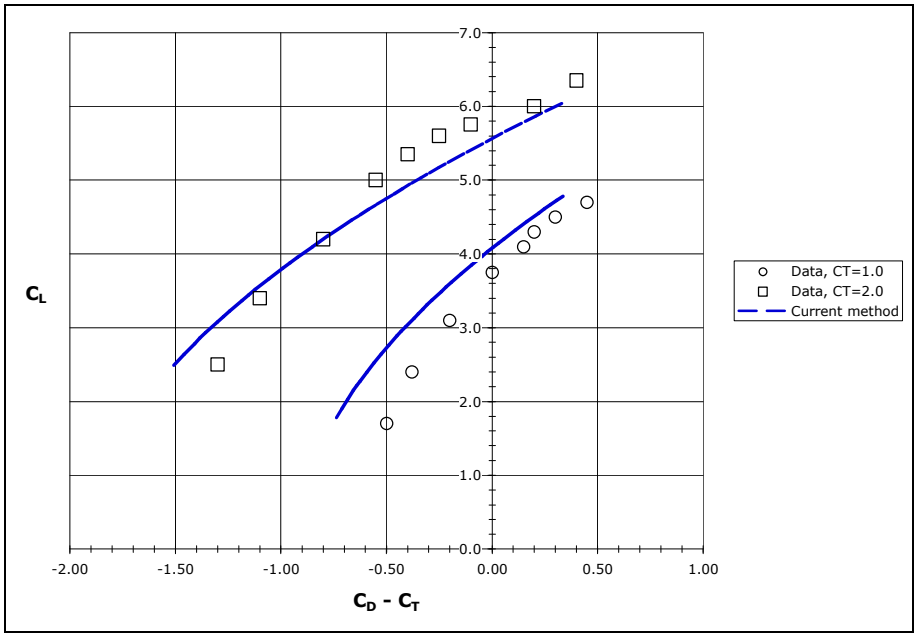

Figure 10. Thrust+Drag polar compared with experiment

B. Comparison withNASA TN D-8061[2]

This set of experiments was done on a small-scale model of a full USB aircraft. The configuration used 4 engines rather than 2 and used rectangular exhaust nozzles. Figure 11 shows a sketch of the wing:

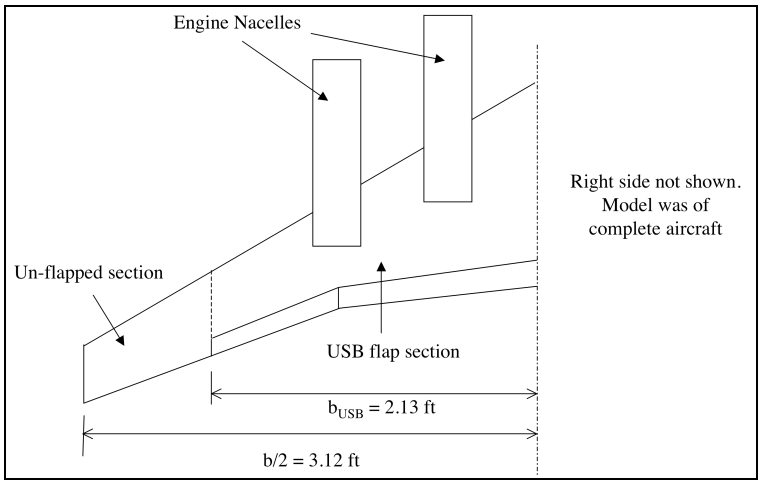

Figure 11. Sketch of wing of USB aircraft model used in Ref. 2

Figures 12 and 13 show comparisons of the predicted values with experimental values for lift and pitching moment, respectively. These plots are for a sample case with 35 degrees USB flap deflection. Note that the lift coefficients agree very well for the range of total thrust coefficients, but the pitching moment agreement is poor. This is due to the effect of the large nacelles located far forward of the aircraft C.G., which contribute a "nose-up" pitching moment.

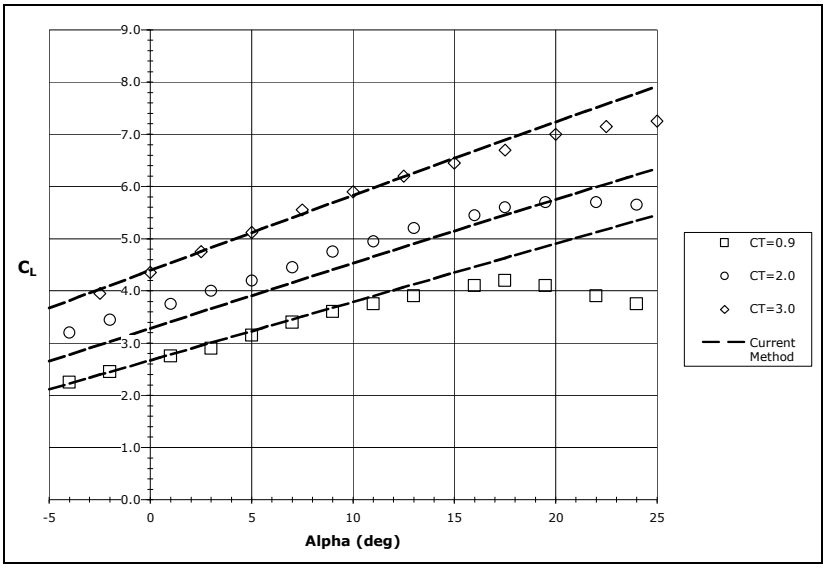

Figure 12. Comparison of C_L with experiment

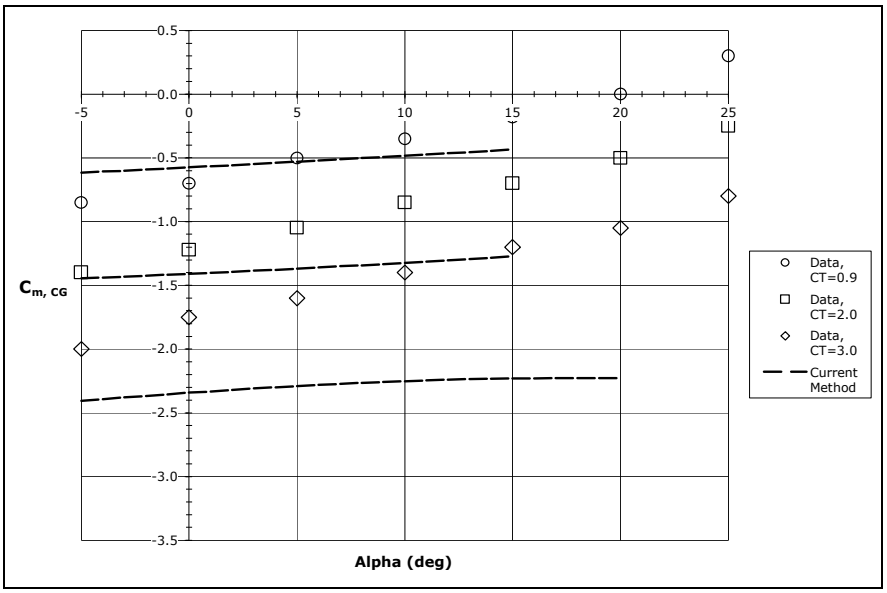

Figure 13. Comparison of $C_{m,CG}$ with experiment

The numerical oscillations encountered in the twin-engine case were still present in the 4-engine configuration, but the wing loading was lower, making the oscillations less severe. As a result, the induced drag was much more reasonable, as shown in Figure 14 for 35 degrees USB flaps at various total thrust coefficients.

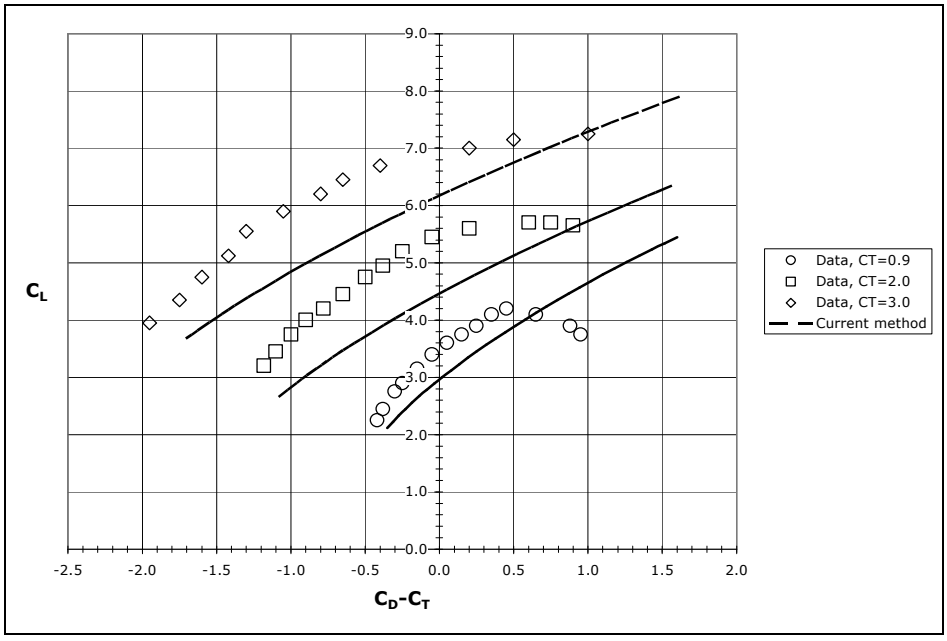

Figure 14. Thrust+Drag polar comparison with experiment

C. Comparison with non-linear VLM

One of the most successful and comprehensive inviscid panel methods for USB was developed by Mendenhall and Spangler[22]. Potential flow models of the lifting surfaces and jet wakes are combined to calculate induced interference on the wings and flaps. The wing/flap model is a non-planar, non-linear, vortex lattice method. The multiple chordwise panels allow the curvature of the USB flap to be modeled as discrete planar portions, analogous to the method used in the current work for 2-D. The jet wake is modeled as a rectangular vortex ring distribution,

whose strength is determined from engine exit conditions and empirical information on the flow in turbulent wall jets.

Since the non-linear VLM was intended to for "stand-alone" use in predicting longitudinal aerodynamic characteristics, corrections were applied to account for the effects of leading-edge devices, nacelles, fuselage, and ram drag. Nacelle and fuselage effects were modeled using slender-body theory. No viscous drag corrections are included in this method, meaning that drag consists only of the induced drag, estimated ram drag, and the axial component of the force generated by the wing. Contributions of the estimated ram drag and engine thrust to pitching moment are included in the VLM method.

Comparisons of the VLM against NASA USB reports were presented in Ref. 22. This VLM method appears to produce good results for C_L and C_m for unswept wings at moderate flap deflections and thrust coefficients. Fortunately, some of the comparisons presented in Ref 22 were for the same cases as those used in the current work. This allows direct comparisons between the methods. Figure 15 shows a comparison of VLM, current method, and experimental data for the model of ref 2 (see Figure 11) at a flap deflection of 45 degrees:

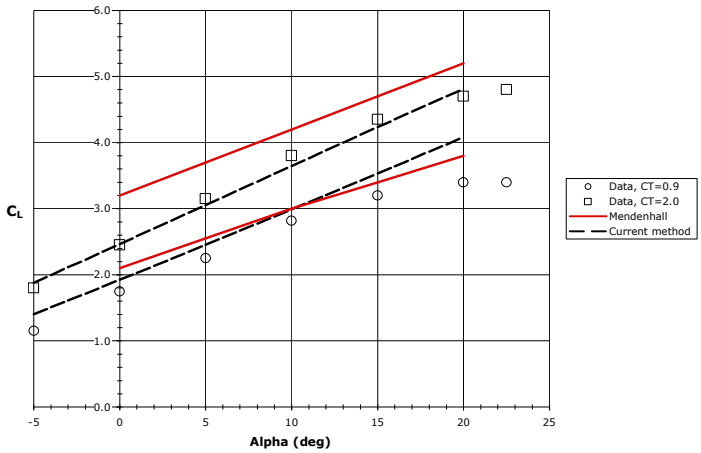

Figure 15: C_L predictions from VLM of Ref. 21 and the current method for 45 deg deflected radius flap at 2 thrust settings

Note that the VLM cannot account for the low turning angle achieved using a radius flap, a factor that is easily accounted for in the current method. For this configuration, the current method provides equivalent or better estimations of both the lift coefficient (always within 15% of experiment for unstalled region) and C_m. Similar to our method the VLM method, based on potential flow, is incapable of predicting stall. Figure 16 shows a comparison of the pitching moments:

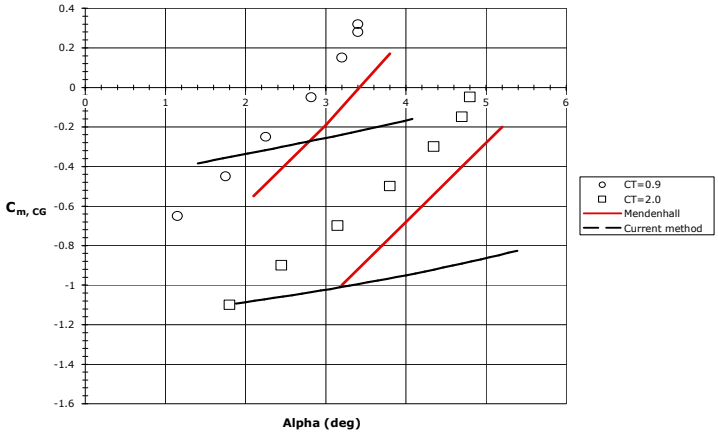

Figure 16: Pitching moments about the C.G. for 45 deg flaps at 2 thrust settings

Notice that the pitching moment slopes (dC_m/dC_L) are clearly not predicted well by the current method, while they are accurately predicted by the VLM. However, recall that this is the same aircraft model used in Figure 11, where the pitching moment slopes are also not predicted well by the current method. The VLM includes corrections

for nacelle, fuselage, and leading-edge slats, while we did not include such corrections. It is found that the CST model provides better estimates of the surface pressures on the flap. CST also provides the important capability to include empirical relations about the turning efficiency of the jet. Thus, the decrease in turning angle of the jet can be modeled well, while VLM can only model losses in thrust due to turning, not the actual angle.

Thus the current method compares favorably to a non-linear, vortex lattice method developed for USB, and has the additional benefit of predicting drag, which is crucial for USB designs. The weaknesses of the current method are typically shared with the VLM, such as the inability to predict stall and the need for empirical information about the jet.

VI. Conclusions

The current methodology agrees well with experimental data for the cases examined. The method, as expected, was sensitive to the propulsive system input. The more accurately exhaust conditions are specified, the more accurate the predictions. Based on the correlation with 2-D data, the overall method becomes less accurate for large blowing coefficients or large flap deflections. Better empirical relations for changes with flap setting and changes in exhaust conditions could improve predictions. However, this methodology will be useful in the early phases of aircraft design.

Acknowledgment

We gratefully acknowledge the support of AVID LLC for suggesting this topic and providing support for us to perform this work.

References:

[1]Wimpress, John K., Newberry, Conrad F., *The YC-14 STOL Prototype: Its Design, Development and Flight Test*, AIAA Case Study, AIAA, 1998.

[2]Sleeman, William C. Jr., Hohlweg, William C., "Low-Speed Wind Tunnel Investigation of a Four Engine Upper Surface Blown Model having a Swept Wing and Rectangular and D-Shaped Exhaust Nozzles", NASA TN D-8061, Dec. 1975.

[3]Riddle, D.W., et al, "Powered-Lift takeoff performance characteristics determined from flight test of the Quiet Short-Haul Research aircraft", AIAA 81-2409, AIAA Flight Testing Conference, Las Vegas, NV, Nov. 1981.

[4]Sussman, M.B., et al, "USB Environment Assesment based on YC-14 Flight Test Measurements", AIAA 77-0593, 1977.

[5]Roberts, D.W., "A Zonal Method for Modeling Powered-Lift Aircraft Flow Fields", NASA CR-177521, March, 1989.

[6]Atta, E., Ragab, S., and Birckelbaw, L., "Euler Solutions for Aircraft Configurations Employing Upper Surface Blowing", *Journal of Aircraft*, Vol. 24, No. 3, May 1985.

[7]Henderson, Campbell, Walters, Marvin, "High-Lift STOL Aerodynamics / Stability & Control Prediction Techniques Assesment", Naval Air Development Center Report 81261-60, March, 1983.

[8]Keen, Ernest B., "A Conceptual Design Methodology for Predicting the Aerodynamics of Upper Surface Blowing on Airfoils and Wings", M.S. Thesis, Virginia Polytechnic Institute and State University, 2004.

[9]Spence, D.A., "The Lift Coefficient of a Thin, Jet-Flapped Wing", *Proc. of the Royal Society of London, Series A*, Vol. 238, Issue 1212, pp 46-68, 1956.

[10]Karamcheti, K., *Principles of Ideal-Fluid Aerodynamics*, John Wiley & Sons, 1966.

[11]Siestrunck, R., "General Theory of the Jet Flap in Two-Dimensional Flow", *Boundary Layer and Flow Control*, Ed. G.V. Lachmann, Vol. 1, pp. 342-364, Pergamon Press, 1961.

[12]Hough, G.R., "A Study of the Blown Flap/Jet Flap Analogy", AIAA 79-0119, 17th Aerospace Sciences Meeting, New Orleans, LA, Jan. 1979.

[13]Spence, D.A., "The Lift on a Thin Aerofoil with a Jet-Augmented Flap", *The Aeronautical Quarterly*, pp. 287-299, August, 1958.

[14]Davis, W.H. Jr., "Extension of Spence's Jet-Flap Theory for Thin Airfoils to account for Camber Effects", Memo EG-ARDYN-79-08, Grumman Aerospace, Jan., 1979.

[15]Mason, William, *Applied Computational Aerodynamics*, 1997.

[16]Torenbeek, Egbert, *Synthesis of Subsonic Airplane Design*, Delft University Press, 1981.

[17]Roberts, C.R., "An Experimental Investigation of a Powered Wing in Two- Dimensions", M.S. Thesis, University of Texas at Arlington, 1984.
[18]Pernice, Ciro, "An Experimental Study of a Two-Dimensional Propulsive Wing", M.S. Thesis, University of Texas at Arlington, 1986.
[19]Jeon, C.S., "Experimental Study of a Two-Dimensional Propulsive Wing in a Low-Speed Wind Tunnel", M.S. Thesis, University of Texas at Arlington, 1990.
[20]Paris, J.K.F., "Advancements in the Design Methodology for Mult-Element High-Lift Systems on Subsonic Civil Transport Aircraft", M.S. Thesis, University of California at Davis, 1999.
[21]Smith, Charles C., Phelps, Arthur E., Copeland, W., "Wind Tunnel Investigation of a Large-Scale Semispan Model with an Unswept Wing and an Upper Surface Blown Jet Flap", NASA TN D-7526, Feb., 1974.
[22]Mendenhall, M.R., and Spangler, S.B., "Calculation of the Longitudinal Aerodynamic Characteristics of Upper Surface Blown Wing-Flap Configurations", NASA CR-3004, 1978.